

## GMR in Granular CuFe with a Face Centered Tetragonal Structure of Iron

J. EBERT (a), M. GHAFARI (a), B. STAHL (a), H. HAHN (a), M. D. MARTINS (b),  
and W. A. A. MACEDO (b)

(a) *Materials Science Department, Thin Films Division,  
Darmstadt University of Technology, Petersenstr. 23, D-64287 Darmstadt, Germany*

(b) *Laboratorio de Fisica Aplicada, CNEN, 31270-010 Belo-Horizonte, Brazil*

(Received May 1, 2001; accepted September 30, 2001)

Subject classification: 75.50.Tt; 75.70.Cn; 75.70.Pa; S1.1; S1.3

Granular thin CuFe films with a face centered tetragonal (fct) structure of Fe clusters in Cu matrix show a giant magnetoresistance effect. The samples were prepared by co-deposition of  $^{57}\text{Fe}$  and Cu metal in Ultra High Vacuum. The role of the scattering of conduction electrons at the interface between Fe ultrafine particles and Cu matrix has been studied by Mössbauer spectroscopy and magnetoresistivity measurements. The ratio of Fe atoms located at Cu/Fe interface and in the ultrafine particles (bulk) was resolved by Mössbauer spectroscopy. In the system consisting of ultrafine fct-Fe particles imbedded in Cu matrix the giant magnetoresistance effect is not correlated to the ratio of interface/bulk in contrast to observations in FeAg granular system. The spin-dependent scattering of conduction electrons occurs within the ferromagnetic fct-Fe particles.

**Introduction** Granular thin films with isolated Fe clusters of few nanometers size embedded in the Cu matrix show giant magnetoresistance effect (GMR). Granular  $\text{Cu}_{100-x}\text{Fe}_x$  can be prepared by co-evaporation of Fe and Cu under UHV conditions. The structure of the iron clusters in Cu matrix is strongly related to the Fe concentration. For  $x > 35$ , the structure of Fe particles in Cu matrix is body centered cubic (bcc) while below  $x < 22$  a face centered cubic (fcc) or face centered tetragonal (fct) have been observed. Fe clusters remain fcc or fct as long as their size is so small to keep the lattice coherency with the Cu matrix. In situ EXAFS measurements during the deposition show that the Fe atoms aggregate together in form of clusters which are intermixed by Cu matrix at the interface. Different orientation of the magnetization of the isolated Fe particles have an influence on the electrical properties and lead to the observed GMR effect. The GMR effect is attributed to the spin dependent scattering of electrons which occurs within the ferromagnetic particles [1, 2] or at interfaces to the non-magnetic metals [2, 3]. It has been conceived [4] that in granular systems with bcc-Fe the interfacial scattering of conduction electrons deforming the magnitude of the GMR effect. However, the influence of interfaces on GMR effect in granular systems with fcc-Fe or fct-Fe has not been investigated. Wakoh et al. [5] have shown that the magnitude of GMR ratio depends on the Fe content and the fabrication methods. According to the theoretical calculations the magnetic ground state of  $\gamma$ -Fe is related to the lattice parameters. Depending on lattice parameters the Fe could be non-magnetic, antiferromagnetic or ferromagnetic [6, 7]. A first order phase transition from antiferromagnetic to ferromagnetic state is predicted at 3.66 Å lattice spacing. The coherent participates in Cu with a lattice parameter of 3.61 Å correspond to  $\gamma$ -Fe with antiferromagnetic state. The fcc magnetic moment is predicted to increase monotonically with

increasing lattice spacing [8]. The fct-Fe are in high-spin state with a ferromagnetic coupling of atoms [9–11]. Because of the low magnetic moment of  $\gamma$ -Fe, the GMR effect is very low (about 1%) [12]. However, Fe clusters with a fct structure show GMR effects up to 23% at low temperatures [5]. The fct-Fe clusters are in a ferromagnetic state with a magnetic hyperfine field distribution. The most probable magnetic hyperfine field (27 T) is about 20% less than  $\alpha$ -Fe at 5 K. Because of the high spin state of the fct-Fe, the study of the magnetoresistance of fct-Fe is advantageous in comparison to fcc-Fe particles.

The aim of the present work is to determine the correlation between the magnetic structure within the nanoparticles and the GMR effect. Especially the role of the interfacial scattering on the GMR effect will be of interest. For this purpose, two representative samples with different Fe concentrations ( $\text{Cu}_{91}\text{Fe}_9$  and  $\text{Cu}_{88}\text{Fe}_{12}$ ) have been studied in detail. Mössbauer spectroscopy as a local probe gives the possibility to reveal the structural and magnetic properties at the different Fe sites in the CuFe system. The local structure of fcc-Fe and fct-Fe atoms and the distribution of Fe in Cu matrix can be identified by the hyperfine interactions [9, 11, 13, 14]. For example, fcc-Fe participants in Cu matrix at room temperature are characterized by a single line with an isomer shift of  $\text{IS} = -0.11$  mm/s relative to  $\alpha$ -Fe and a magnetic hyperfine field of about 2.3 T at 4.2 K. The Fe atoms with 12 Cu atoms as nearest neighbors have a single line with an isomer shift of 0.22 mm/s. A quadrupole splitting (QS) of about 0.64 mm/s and an isomer shift of 0.19 mm/s have been reported for Fe agglomerates consisting of two, three or more atoms [15].

Above the magnetic transition temperature, the local structure of fct-Fe is characterized by an asymmetric quadrupole splitting distribution with an average value of 0.38 mm/s and an isomer shift of  $-0.04$  mm/s. From the Mössbauer parameter it is possible to distinguish between the local atomic environments of the Fe atoms within the Fe particles and Fe atoms located at the interfaces between Cu matrix and Fe particles. In addition, the ratio of Fe atoms in Cu/Fe interface and within particles can be derived from the relative intensity of the Mössbauer spectra.

**Experimental** Clusters of fct-Fe dispersed in Cu matrix with a thickness of about 100 nm were prepared by co-evaporation of Fe and Cu in an ultra high vacuum MBE system with a base pressure of about  $10^{-8}$  Pa. In the present report the results of measurements of two samples with Fe concentrations of 9 at% and 12 at% are presented. An electron mini beam evaporation source with quartz rate monitor and a K-cell were used to co-deposit  $^{57}\text{Fe}$  and Cu, respectively.  $^{57}\text{Fe}$  and Cu were deposited on polyamide substrates with a deposition rate of 0.01 nm/s for Fe and variable rates of 0.1–0.16 nm/s for Cu. The temperature of the substrate during the deposition was about 330 K. The chemical compositions of granular samples were verified by Rutherford backscattering spectroscopy (RBS) and X-ray photoelectron spectroscopy (XPS) measurements. A standard dc four-point technique was used to measure the electrical resistivities at different temperatures and in applied magnetic fields up to 5 T parallel to the film plane and the current direction. Depth-selective conversion electron Mössbauer spectroscopy (DCEMS), integral conversion electron Mössbauer spectroscopy (ICEMS) and transmission Mössbauer spectroscopy were used to determine the microscopic properties. The isomer shift (IS) values given in the present work are relative to bcc-Fe at room temperature.

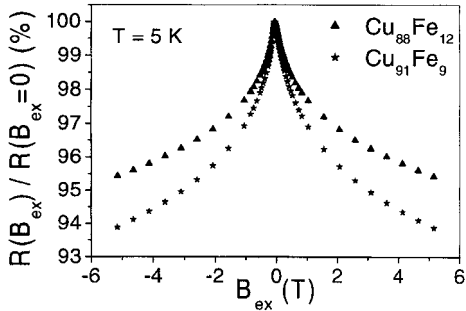


Fig. 1. Electrical resistance  $R(B_{ex})/R(B_{ex} = 0)$  vs. external magnetic field for CuFe films measured at 5 K

In situ XPS analysis of samples in the MBE chamber shows no sign of oxidation. For resistivity and Mössbauer measurements at different temperatures the samples were transferred from the MBE chamber to an ambient atmosphere. The GMR

Mössbauer measurements were performed in He atmosphere.

DCEMS measurements after exposition to the ambient atmosphere show the formation of oxides ( $Fe^{3+}$ ) in a depth of about 2 nm from the top of the surface. The relative intensities of Fe oxide to Fe clusters in a depth of 5 nm is about 50%. The oxidation starts at the interface between Fe and Cu. Because of the low amount of oxidation (about 1%) in comparison to the whole film (100 nm), the influence of oxidation on the GMR is insignificant.

**Results and Discussion**

**Magnetotransport measurements** Figure 1 shows the external field,  $B_{ex}$ , dependence of the relative resistivity  $R_{rel}(B_{ex}) = R(B_{ex})/R_{max}$  at 5 K,  $R_{max}$  is the maximum value of the resistance. The studied FeCu samples did not saturate even at 5 T, therefore the given definition was used. At 5 T a maximum GMR of 7% and 5% was obtained for samples with Fe concentration of 9 at% and 12 at%, respectively. The magnitude of the GMR effect depends on the Fe concentration. In order to understand the concentration dependence of GMR effect in these systems, Mössbauer spectroscopy was used to clarify the atomic structure of the Fe clusters.

**Mössbauer measurements** The Mössbauer spectra and the quadrupole splitting (QS) distribution of granular CuFe samples measured at 300 K are shown in Fig. 2. The details for the determination of the QS distribution are given in Ref. [16]. The Mössbauer spectrum of CuFe with low Fe concentration at room temperature consists of a weak asymmetric QS distribution with an average value 0.38 mm/s. The asymmetry of QS is caused by the relation between IS and QS. Similar to the metallic sys-

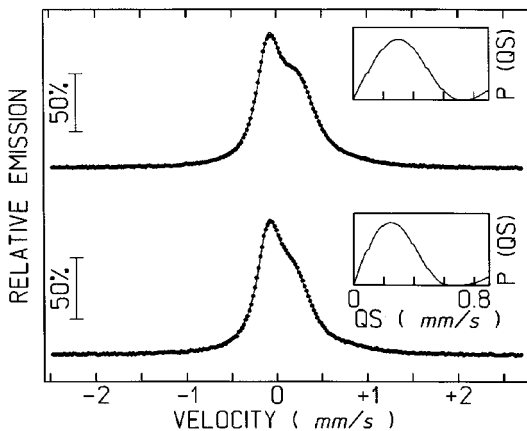


Fig. 2. Mössbauer spectra and quadrupole distributions,  $P(QS)$ , of CuFe granular films measured at 300 K. Top:  $Cu_{91}Fe_9$ ; bottom:  $Cu_{88}Fe_{12}$

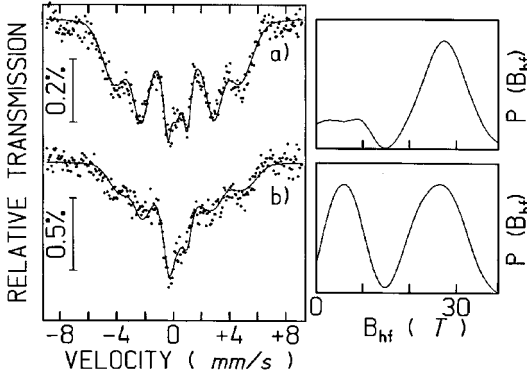


Fig. 3. Mössbauer spectra and the magnetic hyperfine field distributions,  $P(B_{\text{hf}})$ , of granular a)  $\text{Cu}_{91}\text{Fe}_9$  and b)  $\text{Cu}_{88}\text{Fe}_{12}$  samples measured at 5 K

tion of CuFe Films are shown in Fig. 3. The details of the analysis of the magnetic spectra are given in Ref. [18]. The magnetic hyperfine distributions of CuFe samples at 5 K can be deconvoluted into two components: a magnetic hyperfine distribution with a most probable field of 27 T and a low field component with an average magnetic field of 6 T. The average hyperfine field and the form of the low field component are consistent with the Mössbauer parameters of Fe atoms at the interface between Fe and Cu [9]. Therefore, this component is attributed to Fe atoms at the interface between the fct-Fe particles and the Cu matrix. The relative intensities of two components in Mössbauer spectra are related to the Fe concentration in the particles and at the interfaces. For  $\text{Cu}_{91}\text{Fe}_9$  and  $\text{Cu}_{88}\text{Fe}_{12}$  films, the relative intensities of the low field components are 23% and 40%, respectively. From this observation it can be concluded that in CuFe granular films the particle size decreases with increasing Fe concentration. In other words, the increase of the Fe concentration results in an increase of the interface/bulk ratio. This conclusion is confirmed by the relaxation phenomena in these systems. The fct-Fe clusters are single domains with sizes of few nanometers. The clusters are in a superparamagnetic state. Above a defined temperature known as blocking temperature the magnetic hyperfine interaction disappears. In the superparamagnetic state the magnetization anisotropy energy is comparable to the thermal energy. The magnetization direction fluctuates between the energy minima with a relaxation time,  $\tau$ , given by

$$\tau = \tau_0 \exp(\Delta E/kT). \quad (1)$$

The pre-exponential factor  $\tau_0$  is of the order  $10^{-9}$ – $10^{-11}$  s. The energy barrier between two magnetization directions,  $\Delta E$ , is determined by the magnetic anisotropy energy and the volume of the particles. The time scale,  $\tau$ , which is required for the magnetic hyperfine interactions in the case of Mössbauer spectroscopy is about  $\tau = 10^{-8}$  s. Above the blocking temperature at which the magnetic hyperfine interactions are not resolved, a single line or a QS should be observed. Below the blocking temperature the magnetization vector fluctuates in directions close to the easy direction of magnetization (collective magnetic excitations) [16] with a time scale shorter than  $10^{-8}$  s. The observed magnetic hyperfine field of small particles below the superparamagnetic state is an average magnetic hyperfine field, which is smaller than the magnetic hyperfine field of a bulk sample. The measured magnetic hyperfine field,  $B_{\text{hf}}$ , is given by [19]

$$B_{\text{hf}} = B_0[1 - 1/2(k_B T/KV) - 1/2(k_B T/KV)^2 - 5/4(k_B T/KV)^3 - 37/8(k_B T/KV)^4], \quad (2)$$

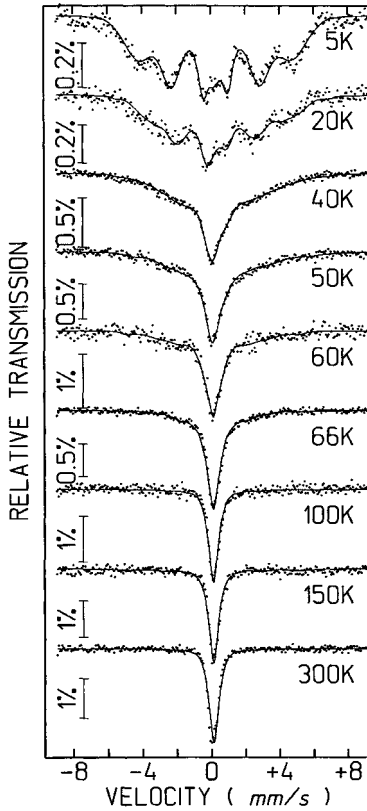


Fig. 4. Mössbauer spectra of  $\text{Cu}_{91}\text{Fe}_9$  film vs. temperature measured in zero external field

where  $B_{\text{hf}}$ ,  $B_0$ ,  $k_B$ ,  $K$  and  $V$  are the measured hyperfine field, the hyperfine field in the absence of the fluctuations, the Boltzmann constant, the anisotropy constant, and the volume of the particle, respectively.

The Mössbauer spectra of the  $\text{Cu}_{91}\text{Fe}_9$  films and the average hyperfine field as a function of temperature are shown in Figs. 4 and 5. Due to the collective magnetic excitations, the average magnetic hyperfine field of small Fe particles decreases linearly with increasing temperature. According to Eq. (2) the energy barrier between easy directions can be estimated from the decrease of the average hyperfine field with temperature. The average hyperfine field at every temperature is a superposition of the collective magnetic excitations of particles and temperature dependence of magnetization (for example spin waves, temperature dependence of spontaneous magnetization, Brillouin function). In order to determine  $KV$ , the magnetic hyperfine field of bulk sample without collective magnetic excitations should be known. The temperature dependence of the average hyperfine field of fct-Fe bulk samples [10] between 4.2 and 60 K shows a decrease of about 5.5 T. Assuming a linear decrease of the hyperfine field of bulk samples with increasing temperature in the range  $4.2 \text{ K} \leq T \leq 60 \text{ K}$ , the ratio of the magnetic hyperfine field of particle,  $B_{\text{hf}}$  (particle), to the magnetic hyperfine field of bulk,  $B_{\text{hf}}$  (bulk), was plotted as a function of temperature in Fig. 6.

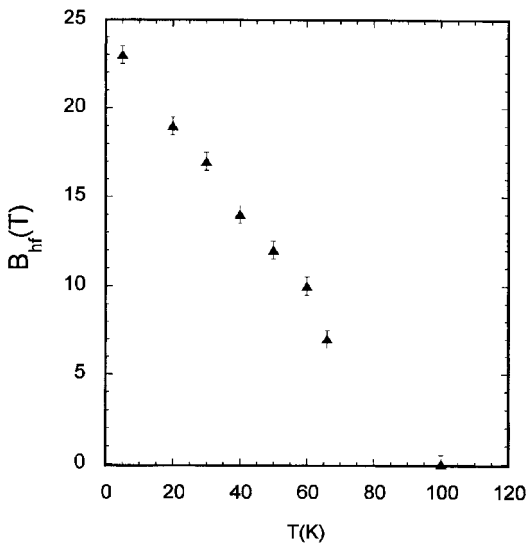


Fig. 5. Average magnetic hyperfine field of granular  $\text{Cu}_{91}\text{Fe}_9$  film vs. temperature

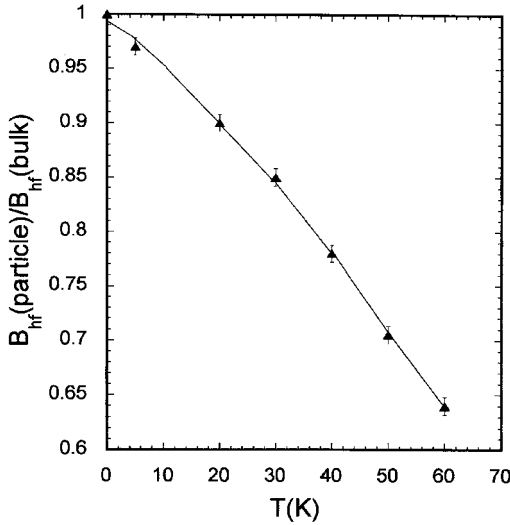


Fig. 6. Ratio of the magnetic hyperfine field of particles,  $B_{\text{hf}}(\text{particle})$ , to the magnetic hyperfine field of bulk,  $B_{\text{hf}}(\text{bulk})$ , vs. temperature

The assumption of a decrease of the magnetic hyperfine field as a function like  $T^2$  or  $T^{3/2}$  does not change the value of energy barrier in essential manner. The best fit of data in Fig. 6 with Eq. (2) was achieved for a value of the energy barrier of  $KV = 1.5 \times 10^{-2}$  eV.

The derived energy barrier is an average value which describes the temperature dependence of the hyperfine field in zero external field. Because of

the size distribution of the magnetic particles, there exists a probability for the small particles to fluctuate between the easy directions at temperatures below the blocking temperatures. As a consequence of the size distribution of the magnetic particles, the relaxation time and the blocking temperature are not well defined. The relaxation time exponentially depends on the particle size (Eq. (1)). At 100 K, however, all the particles are in a superparamagnetic state. Above the blocking temperature,  $T_B = 100$  K, the Mössbauer spectra consist of a paramagnetic component. The fct-Fe clusters with large particles show a ferromagnetic spectrum even at 300 K [9].

The Mössbauer spectra of  $\text{Cu}_{88}\text{Fe}_{12}$  and  $\text{Cu}_{91}\text{Fe}_9$  samples at 66 K are shown in Fig. 7. The Mössbauer spectrum of  $\text{Cu}_{91}\text{Fe}_9$  film consists of a broad unresolved magnetic component and a paramagnetic component. The Mössbauer spectrum of the  $\text{Cu}_{88}\text{Fe}_{12}$  sample, however, shows only a paramagnetic component. This shows a faster relaxation time of  $\text{Cu}_{88}\text{Fe}_{12}$  film in comparison to the  $\text{Cu}_{91}\text{Fe}_9$  sample. In agreement with former measurements the fast relaxation of the magnetization directions in  $\text{Cu}_{88}\text{Fe}_{12}$  film can be interpreted as a consequence of the lower particle size of  $\text{Cu}_{88}\text{Fe}_{12}$  sample in comparison to the  $\text{Cu}_{91}\text{Fe}_9$  films.

Above the the superparamagnetic state (150 K), the magniitude of GMR effect in an external field of 5 T is about 3%. The spin-relaxation process in every particle changes the occupancy of spin up and spin down of Fe 3d electrons. Similar to the multilayers with GMR effect [20], after the reorientation with relaxa-

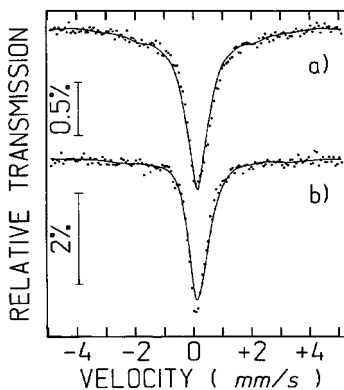


Fig. 7. Mössbauer spectra of a)  $\text{Cu}_{91}\text{Fe}_9$  and b)  $\text{Cu}_{88}\text{Fe}_{12}$  samples measured at 66 K

tion times faster than  $10^{-8}$  s, the majority electrons of 3d band with spin up become the minority electrons of the Fe 3d bands with spin down, and the minority Fe 3d electrons with spin down become the majority electrons with spin up. Because of the different orientation of spins in the particles, the GMR effect can be explained in the framework of the anisotropic scattering of electrons with spin up and down within the ferromagnetic particles. The decrease of GMR magnitude with increasing temperature is explained in the terms of electron–magnon scattering and inelastic scattering by phonons [21].

**Relation of the interface/bulk ratio to the magnitude of GMR** The increasing interface/bulk ratio leads to a decrease of the magnitude of GMR effect in fct-Fe granular systems. This shows that the magnitude of the GMR effect is not affected by the interfacial scattering of the conduction electrons. This trend is caused by the weak magnetic moment of Fe atoms at the interfaces. The average value of magnetic hyperfine fields of 6 T at the interfaces proves that in granular fct-Fe systems, the Fe atoms at the interface between fct-Fe and Cu matrix are magnetically weak. This results in a moderate spin dependent scattering at the interfaces. On the other hand, the increase of Fe concentration in CuFe systems causes an increase of the intermixing between Cu and Fe. This leads to an increase of the thickness of the interfaces between Cu and Fe. The weak magnetic interfaces form a barrier between the Cu matrix and the ferromagnetic fct-Fe clusters which results in an additional scattering of electrons. The additional scattering causes a decrease of the spin dependent scattering within the fct-Fe clusters. In opposite to the fct-Fe particle, the Fe moments at the interface between bcc-Fe particles and Cu or Ag matrix are about 3% less than bulk  $\alpha$ -Fe. In this case the spin dependence of scattering at the interface between Cu and bcc-Fe plays the predominant role for the GMR effect. In fct-Fe clusters, however, the interface between Fe and Cu is a scattering center for all electrons. The spin dependent scattering occurs within Fe clusters. The increase of the interfaces reduces the number of electrons with a spin dependent scattering. The result is a decrease of the magnitude of GMR effect with increasing cluster size.

**Conclusion** The results of Mössbauer spectroscopy and GMR measurements show that the spin dependent scattering at interfaces is determined by the magnitude of magnetic moments of the interface atoms. The weakly magnetic or non-magnetic interfaces form additional scattering centers for the electrons and thus cause a decrease of the GMR effect. For the magnitude of GMR effect, the magnetic state of the interfaces is the dominant factor.

## References

- [1] A.E. BERKOWITZ, J.R. MITCHELL, M.J. CAREY, A.P. YOUNG, S. ZHANG, F.E. SPADA, F.T. PARKER, A. HÜTTEN, and G. THOMAS, Phys. Rev. Lett. **68**, 3745 (1992).
- [2] J. BASS and W.P. PRATT, J. Magn. Magn. Mater. **200**, 274 (1999).
- [3] J.Q. XIAO, J.S. JIANG, and C.L. CHIEN, Phys. Rev. Lett. **68**, 3749 (1992).
- [4] C. ALOF, B. STAHL, M. GHAFARI, and H. HAHN, J. Appl. Phys. **88**, 4212 (1999).
- [5] K. WAKOH, T. HIHARA, T.J. KONNO, K. SUMIYAMA, and K. SUZUKI, Mater. Sci. Eng. A **217/218**, 326 (1996).
- [6] V.L. MORUZZI, P.M. MARCUS, and J. KÜBLER, Phys. Rev. B **39**, 6957 (1989).
- [7] M. UHL, L. M. SANDRASTSKI, and J. KÜBLER, J. Magn. Magn. Mater. **103**, 314 (1992).

- [8] T. KRAFT, P. M. MARCUS, and M. SCHEFFLER, *Phys. Rev. B* **49**, 11511 (1994).
- [9] W. KEUNE, A. SCHATZ, R. D. ELLERBROCK, A. FUEST, K. WILMERS, and R.A. BRAND, *J. Appl. Phys.* **79**, 4265 (1996).
- [10] K. SUMIYAMA, K. NISHI, Y. NAKAMURA, V. MANNS, B. SCHOLZ, M. PRIVIK, W. KEUNE, W. STAMM, G. DUMPICH, and E.F. WASSERMANN, *J. Magn. Magn. Mater.* **96**, 329 (1991).
- [11] A.P. KURIN, L. CHENG, D.W. LEE, Z. ALTOUNIAN, and D.H. RYAN, *J. Appl. Phys.* **85**, 5738 (1999).
- [12] O. DURAND, J.M. GEORGE, J.R. CHILDRESS, S. LEQUIEN, A. SCHUHL, and A. FERT, *J. Magn. Magn. Mater.* **121**, 140 (1993).
- [13] T. EZAWA, W.A.A. MACEDO, U. GLOS, W. KEUNE, K.P. SCHLETZ, and U. KIRSCHBAUM, *Physica B* **161**, 281 (1989).
- [14] V. KUNCSEK, M. ROSENBERG, A.R. YAVARI, and G. FILOTI, *J. Alloys Compd.* **289**, 270 (1999).
- [15] K. KIRISCHEL, S. NASU, U. GONSER, W. KEUNE, J. LAUER, and D.L. WILLIAMSON, *J. Phys. (France)* **41**, C1-417 (1980).
- [16] G. LE CAER and J.M. DUBOIS, *J. Phys. E* **12**, 1083 (1989).
- [17] M. GHAFARI, U. GONSER, H.G. WAGNER, and M. NAKA, *Nucl. Instrum. Methods* **199**, 197 (1982).
- [18] R.A. BRAND, J. LAUER, and W. KEUNE, *Phys. Rev. B* **31**, 1630 (1985).
- [19] S. MØRUP, *J. Magn. Magn. Mater.* **37**, 39 (1983).
- [20] I. MERTIG, in: *Magnetismus von Festkörpern und Grenzflächen*, 24. IFF-Ferienkurs (1993).
- [21] A. FERT and L. PIRAUX, *J. Magn. Magn. Mater.* **200**, 338 (1999), and references therein.